

**Formaldehyde-isobutene Prins condensation over MFI-type zeolites**

Journal:	<i>Catalysis Science & Technology</i>
Manuscript ID	CY-ART-08-2018-001667.R1
Article Type:	Paper
Date Submitted by the Author:	21-Sep-2018
Complete List of Authors:	Vasiliadou, Efterpi; University of Delaware, Department of Chemical and Biomolecular Engineering, Catalysis Center for Energy Innovation Sha, Li; University of Delaware, Department of Chemical and Biomolecular Engineering, Catalysis Center for Energy Innovation Caratzoulas, Stavros; University of Delaware, Chemical Engineering Lobo, Raul; University of Delaware, Department of Chemical Engineering; University of Delaware

Formaldehyde-isobutene Prins condensation over MFI-type zeolites

Efterpi S. Vasiliadou^a, Sha Li^a, Stavros Caratzoulas^a, Raul F. Lobo^{a,b,*}

^aDepartment of Chemical and Biomolecular Engineering, Catalysis Center for Energy Innovation, University of Delaware, 221 Academy Street, Newark, DE, United States

^bCenter for Catalytic Science and Technology, Department of Chemical and Biomolecular Engineering, University of Delaware, Newark, DE, United States

Corresponding author e-mail address: lobo@udel.edu

Abstract

The liquid phase Prins condensation of formaldehyde with butenes on H-ZSM-5 (MFI) zeolite catalysts was investigated showing that reaction rates follow the order isobutene > 1-butene > cis-2-butene. The catalytic rates for medium-pore zeolite H-ZSM-5 were not only a larger than for H-beta, but also selective for of 3-methyl-3-buten-1-ol during formaldehyde condensation with isobutene. Isoprene forms, under the optimal reaction conditions, either in a second dehydration step of the unsaturated alcohol, or in a single step over H-ZSM-5 with optimal Si/Al ratio (Si/Al=40). Mechanistic studies revealed that sequential Prins cyclization and hetero-Diels-Alder reactions of the desired products, forming six carbon species, occur only at slow rates over H-ZSM-5. Using DFT methods it was determined that the reaction follows a two-step mechanism: protonation of formaldehyde and electrophilic attack to the alkene, and deprotonation of the resulting intermediate carbocation. For isobutene and 1-butene, the electrophilic addition is coordinated with the protonation of the formyl group, but for cis-2-butene, it is coordinated with the proton back-donation step. The rate-limiting step switches from electrophilic addition for isobutene to proton elimination for the other two C4 isomers.

Keywords: Prins condensation, formaldehyde, isobutene, H-ZSM-5 zeolite, Brønsted acid site

1. Introduction

Branched five-carbon unsaturated alcohols are attractive synthetic targets because they are excellent precursors to fine chemicals, but also starting compounds for the production of commodity chemicals such as dienes. They are valuable as fuel additives, due to their high-octane number and have excellent combustion and anti-knock properties.¹⁻³ These molecules, and specifically 3-methyl-3-buten-1-ol (Scheme 1 compound **I**), are used in the fragrance industry, in pharmaceuticals, agrochemicals and polymers.⁴ In particular isoprene (**IV**), was easily formed by the dehydration of **I**; an important monomer for the preparation of synthetic rubbers (polyisoprene rubber, butyl rubber, styrene or acrylonitrile co-polymers).

Currently, isoprene is primarily obtained as a by-product from the five-carbon fraction of naphtha steam cracking; however, the yields are usually low.⁵ In fact, isoprene production is decreasing due to the shift from naphtha to ethane steam crackers as shale-gas-derived ethane has become widely available and inexpensive. Prins condensation of formaldehyde with isobutene (Scheme 1) has been used as an on-purpose method to isoprene.⁵⁻¹³ Prins condensation is also a powerful tool to form numerous useful products; for instance condensation of formaldehyde with β -pinene over metal organic frameworks (MOFs) to form nopol, a very useful product in agrochemical industry.¹⁴ The reaction of formaldehyde with isobutene can be carried out in one or two steps: the first stage of the more common two-step process requires a liquid-phase catalysis (aqueous sulphuric acid or phosphoric acid) for the reaction of formaldehyde with isobutene to form 1,3-dioxane, 4,4-dimethyl (Scheme 1, **III**). In a second step, **III** decomposes to form isoprene and formaldehyde over calcium phosphate in the vapour-phase. This process suffers from high capital costs and the use of corrosive mineral acids. The single-step process has been investigated in the vapor phase with solid catalysts such as zeolites, phosphates, sulfates, mixed metal oxides and heteropoly acids. Dang et al.¹² have shown that high isoprene yield (63% based on formaldehyde) can be obtained in the presence of $\text{CuSO}_4/\text{SiO}_2$ doped with MgO and at high isobutene to formaldehyde ratios (> 6.0). $\text{V}_2\text{O}_5\text{-P}_2\text{O}_5$ ⁹ is efficient in the vapour phase at 513K and yields of up to 50% have been obtained. These catalysts, however, deactivate quickly.

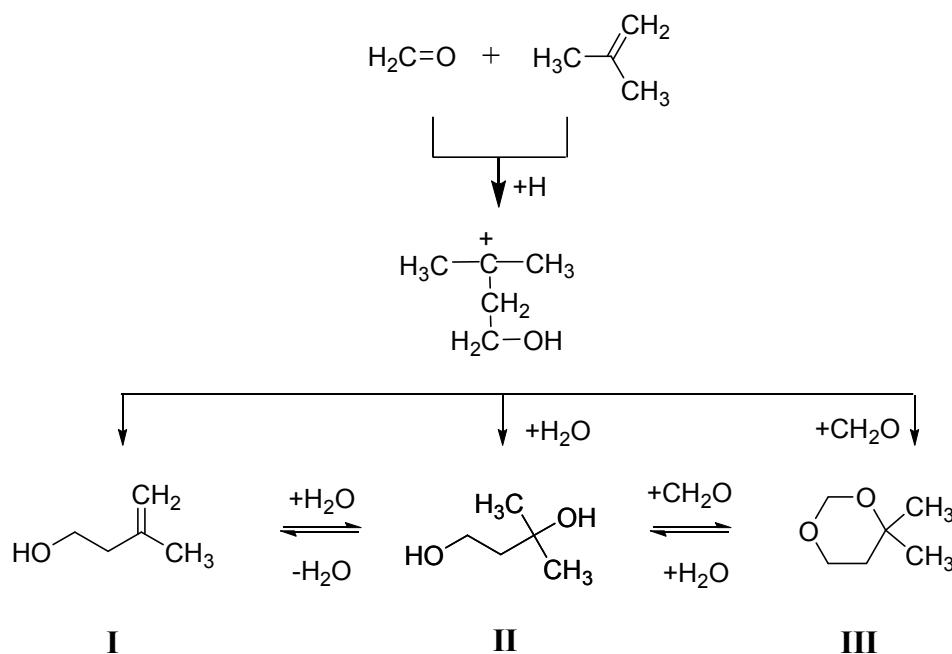
Sushkevich et al.¹⁵ have reported that 20wt% of the heteropolyacid $\text{H}_3\text{PW}_{12}\text{O}_{40}$ supported on silica yields 48% of isoprene (63% selectivity) at 543-563K for an isobutene to formaldehyde ratio of 7.0. High concentration of weak Brønsted acid sites was crucial for obtaining high isoprene selectivity. The active sites for isoprene formation were unsaturated branched surface species

over weak Brønsted sites. Dumitriu group investigated zeolites as catalysts for Prins condensation of formaldehyde with isobutene (formed in-situ via *t*-butanol dehydration) using a pulse microreactor.^{10,11} They tested a series of zeolites (HY, USY, H-ZSM-5, H-B-silicalite) as well as H-B-MCM-41 and found that strongly acidic USY and H-ZSM-5 are not selective for isoprene because pore size and especially acid strength influence selectivity. They proposed that high selectivity to isoprene requires weak acid sites so that formaldehyde protonation prevails over isobutene protonation, limiting side reactions of the olefin.

Previous research has shown that isoprene formation proceeds through either decomposition of **III** (Scheme 1) or hydrolysis of the latter to 1,3-butanediol, 3-methyl (Scheme 1, compound **II**) and further dehydration of the alkanediol. Key parameters were the presence of water in the feed and the application of relatively high temperatures (>513K) to achieve decomposition of the alkyl-m-dioxane as well as dehydration of the 1,3-diol. We identified only one example describing a process where acetic acid is used as a solvent and reactant over Sn/MCM-48; in this case, however, the acetate was selectively formed and its hydrolysis to **I** was needed.¹⁶ On the other hand, significant work targeting 3-methyl-3-buten-1-ol (**I**) as the most desired product has been disclosed in patents.¹⁷⁻²⁰ For instance, 3-methyl-3-buten-1-ol can form selectively from formaldehyde and isobutene using either sodium hydrogen phosphate or a transition metal salt at 423-523K for the former and at 573-633K for the latter catalyst.^{17,19} In a previous report,²¹ we found that at low temperatures (423K) and under anhydrous conditions, Prins condensation of formaldehyde with propylene over H-ZSM-5 selectively forms 3-buten-1-ol (using paraformaldehyde as formaldehyde source). Under the same conditions, in a second step, 3-buten-1-ol dehydration to 1,3-butadiene is very facile reaching 46% yield. Thus far, however, a simple, low-temperature, selective process with heterogeneous acid catalysts to form **I**, or isoprene by dehydration of **I**, has not been identified.

We investigated the condensation of formaldehyde and isobutene using zeolite catalysts and found high selectivity to **I** within a low-temperature range (323-348K). We also identified that H-ZSM-5 (MFI) is an extremely efficient catalyst for the formation of 3-methyl-3-buten-1-ol. The reaction mechanism was elucidated by electronic structure theory calculations: the step-wise reaction proceeds via a carbocation intermediate and the electrophilic addition step leading to the carbocation formation is rate limiting. The rate-limiting step, however, becomes the proton elimination from the carbocation intermediate for two other less reactive isomers, 1-butene and cis-2-butene. Isobutene was found to be the most reactive of the three isomers and was the

focus of our experimental efforts thereafter. The Si/Al ratio had a significant impact on product selectivity; at the optimal Si/Al ratio, the I dehydration rate is high enough to form isoprene in a single step at 423K. Investigation of C_4H_8/CH_2O molar ratio, reaction temperature and reactants/catalyst ratio let us identify optimal process conditions. To the best of our knowledge, this is the first time the reaction mechanism over Brønsted acids is unravelled and evidence of selective formation of I via formaldehyde condensation with isobutene and of the formation of isoprene in a one-step process at low temperatures over zeolites.



Scheme 1 Prins condensation of formaldehyde with isobutene

2. Experimental Section

2.1 Catalysts and Catalyst evaluation

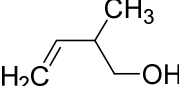
The zeolite catalysts investigated (ZSM-5 (CBV 5524G, Si/Al=25, CBV 8014, Si/Al=40 and CBV 28014, Si/Al=140) and beta (CP814E*, Si/Al=12.5)) were purchased from Zeolyst International in their ammonium form. The acid form was obtained after calcination at 773K for 20h under 100ml/min air flow in a furnace (Thermo Scientific, Lindberg Blue M). Nitrogen physisorption was performed in a Micromeritics 3Flex system at 77 K to determine the micropore volume using the t-plot method.

Samples were degassed overnight at 523K and backfilled with dry nitrogen prior to analysis. X-ray fluorescence (XRF) using a Rigaku WDXRF was used for elemental analysis.

The reaction of formaldehyde with isobutene was carried out in a 50ml batch reactor (4791-93 GP, Parr Instrument Company) under magnetic stirring. The temperature was controlled with a band heater and a controller (Dwyer Instruments, Inc.). In a typical experiment, the reactor was loaded with required amounts of the reactants (paraformaldehyde-Sigma-Aldrich was used as a source for formaldehyde), solvent (1,4-dioxane anhydrous 99.8%, Sigma-Aldrich=20 ml) and an appropriate amount of catalyst. Isobutene (100g, Sigma-Aldrich) was liquefied using an acetonitrile-dry ice bath and added to the reactor containing the solvent. Reaction temperature was set at 423K unless otherwise stated. After reaction, the reactor was cooled down using an ice bath. The gas phase was collected using a gas bag and the liquid phase was collected after catalyst separation by filtration. The gas phase was analysed using an Agilent 7890A gas chromatographer equipped with an HP-PLOT Q column (30m length and 0.53mm diameter) and an FID detector. Liquid phase was analysed using an Agilent 7890B gas chromatographer equipped with an Innowax column (30m length and 0.25mm diameter) and an FID detector as well. Liquid products were also identified with gas chromatography (GC)-mass spectroscopy (MS) using a Shimadzu GC-2010 having the same Innowax column coupled with a GC-MS-QP2010 PLUS. Reaction products were quantified using the multiple point external standard method. Products will be abbreviated as show in Table 1.

Table 1 Compounds chemical structure and abbreviations

Compound name	Structure	Abbreviation
3-methyl-3-buten-1-ol		I
1,3-butanediol, 3-methyl		II
1,3-dioxane, 4,4-dimethyl		III
isoprene		IV
2H-pyran, 3,6-dihydro-4-methyl		V
3-methyl-2-buten-1-ol		VI
3-penten-1-ol (E)		VII

3-penten-1-ol (Z)		VIII
2-methyl-3-buten-1-ol		IX

Conversion of formaldehyde was calculated based on products and reaction stoichiometry using the equation:

$$\text{Conversion} = \frac{\text{moles of } CH_2O \text{ converted to all products}}{\text{moles of } CH_2O \text{ initially loaded}}$$

Selectivity was carbon-based excluding tert-butanol formed via isobutene hydration (specific details for this reaction are given below and discussed where needed) and product yield was calculated based on initial formaldehyde:

$$C - \text{based selectivity} = \frac{\text{moles of } C \text{ in product } i}{\text{moles of } C \text{ in all products}}$$

$$\text{Product Yield} = \frac{\text{moles product } i}{\text{moles of } CH_2O \text{ initially loaded}}$$

2.2 Computational Method

The H-ZSM5 model was constructed by substituting Al in the T12 position of the MFI unit cell and by adding a proton to an adjacent oxygen atom in the lowest-energy configuration.²² A cluster of 162 tetrahedral atoms (162T) was cut from the H-ZSM5 crystal and the dangling Si- bonds were saturated with hydrogen atoms in the direction of the Si-O bonds of the crystal and length of 1.47 Å. Three ONIOM layers were then built from coordination spheres of tetrahedral atoms surrounding the T12 site; the high-theory layer (25T) was treated at the M06-2X/6-311G(2df,p) level of theory. The intermediate layer (46T) was treated at the M06-2X/3-21G level of theory; the real layer (91T) was treated with the universal force field (UFF) molecular mechanics theory²³⁻²⁶ The small layer of the model was allowed to relax while the intermediate and outer layers were frozen to maintain the integrity of the zeolite framework structure. We should note that, in preliminary studies, relaxation of the intermediate layer occasionally converged to structures with multiple imaginary frequencies. This ONIOM-based model has been benchmarked²⁷ and successfully used in previous mechanistic studies in zeolites.²⁸⁻³¹ Ground and transition states were characterized by frequency analysis and all transition states were further

validated by intrinsic reaction coordinate (IRC) calculations. All reported energies are corrected for the basis set superposition error. The thermal corrections to the energy have been computed within the harmonic oscillator approximation. The model is shown in Figure S1.

3. Results and Discussion

3.1 Catalyst characterization

The catalysts investigated were characterized using nitrogen physisorption and X-ray fluorescence spectroscopy (Table 2). The micropore volumes of the samples were consistent with the structure of the zeolites with the exemption of H-ZSM-5(140) that shows lower micropore volume. The Si/Al ratio measured by XRF is close to the nominal value for low Si/Al ratios and shows a small deviation for higher Si/Al ratios.

Table 2 Micropore volume and chemical composition (XRF) of zeolite catalysts investigated

Catalyst	Micropore volume (cm ³ ·g ⁻¹)	Si/Al molar
H-beta(19.0) ^[a]	0.21	20.3
H-ZSM-5(25)	0.12	24.4
H-ZSM-5(40)	0.11	36.0
H-ZSM-5(140)	0.04	127.0

[a] Number in the parenthesis indicate nominal Si/Al values

3.2 Prins condensation of formaldehyde with isobutene

The Prins condensation of formaldehyde with isobutene is an acid catalyzed addition of an aldehyde to an alkene.³² The outcome of the reaction depends on reaction conditions (Scheme 1). In a dry solvent, the cationic intermediate generated by the electrophilic addition of formaldehyde loses a proton to generate the unsaturated alcohol **I**. With water and a protic acid, the reaction product is the diol **II**. With formaldehyde in excess and a low reaction temperature the main product is **III**. We have recently shown that H-ZSM-5 catalyzes selectively the reaction of formaldehyde with propylene forming 3-buten-1-ol.²¹ Initially here, t-butanol was utilized as a source of isobutene to explore the possibility of preparing renewably **I** and **IV** (isobutene can be synthesized from ethanol³³); t-butanol also served as a convenient solvent.

Table 3 Conversion and selectivity for the t-butanol and formaldehyde reaction. Catalyst: H-ZSM-5(40), T=423K and 453K, $t_r=1h$, $C_4H_{10}O/CH_2O$ molar ratio=77.5, TON was calculated based on the sum of product moles and the number of acid sites

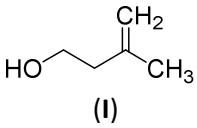
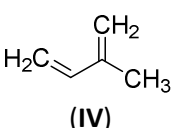
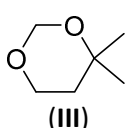
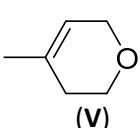
Temperature (K)	CH ₂ O Conversion (%)	TON	Carbon-based Selectivity (%)			
						
423	40.4	12.3	84.8	5.0	8.3	1.9
453	49.8	14.6	76.9	7.7	8.0	7.4

Table 3 compares the reactivity and selectivity at two different temperatures, 423 and 453K. A control experiment using only t-butanol over H-ZSM-5(40), carried out to investigate the dehydration reaction (not shown) led to ~22% dehydration to isobutene. Even at temperatures as low as 423K, the dehydration-condensation cascade is feasible; **I** is the predominant product with 84.8% selectivity at a formaldehyde conversion of about 40%. This example was experimental evidence showing that low-temperature, selective formation of the unsaturated alcohol **I** is attainable. Dehydration of **I** to **IV** also occurs, but the selectivity to **IV** is low (5.0%). **III** and **V** also form, but the selectivity to these six-carbon species is low. Increasing the temperature to 453K to favor dehydration of t-butanol to isobutene and the formation of **I** to **IV**, had no pronounced effect. Instead, using t-butanol as a source of isobutene leads to etherification side products such as propane, 1-(1,1-dimethylethoxy)-2-methyl- (Figure S2), identified by GC-MS. From these observations, we conclude that t-butanol is a potential renewable isobutene precursor,³⁴ but only provided that side reactions are minimized.

Table 4 compares the reactivity of H-ZSM-5 with different Si/Al ratios for the reaction of formaldehyde and isobutene. A control experiment (without catalysts) showed that the reaction does not proceed thermally at 423 K as no Prins condensation products were detected by gas chromatography. On the other hand, the reaction is clearly catalyzed by H-ZSM-5; the latter proved to be a very active and selective catalyst for the Prins condensation. In addition, use of isobutene instead of t-butanol is preferred, as undesired etherification side reactions were not observed. On H-ZSM-5(25), formaldehyde conversion is 43.8% and **I** is the predominant product with selectivity reaching 80%. **IV** was produced

with selectivity 7.8%, in addition to six-carbon products (**III** and **V**). However, the route leading to six-carbon species is very low over H-ZSM-5. Isobutene hydration is a considerable side reaction, producing t-butanol (13.2% yield). This reaction is undesired because it decreases the isobutene available for Prins condensation, but since water forms from dehydration of **I** to **IV** and, to some extent, paraformaldehyde decomposition to formaldehyde monomer hydration reaction cannot be completely eliminated. These data (Table 4) clearly show that the medium-pore H-ZSM-5 catalyzes the selective formation of **I** as opposed to six-carbon products.

In contrast to H-ZSM-5, H-beta is not an efficient catalyst for the Prins condensation of formaldehyde with isobutene since formaldehyde conversion was moderate (18.0%). **V**, formed either by Prins cyclization of **I** with formaldehyde or by Hetero-Diels-Alder of **IV** with formaldehyde (see Scheme 2),²¹ is the predominant product (55.9% selectivity) with zeolite beta. **IV** is the second product having 44.1% selectivity. **IV** could potentially form from several precursors (**I**, **II** and **III**, Scheme 1) through simple or double hydration and decomposition, respectively—however, none of these compounds was detected. It is conceivable that **I** is the intermediate on the way to **IV** because the reaction temperature is quite low (423K) for double dehydration of **II** and decomposition of **III** (temperatures for these reactions are usually higher than 523K^{10,35}). H-beta additionally catalyzes a number of undesired reactions: isobutene hydration was the most considerable one, producing t-butanol (17.0% yield). Other unidentified peaks at lower retention times were also detected by gas chromatography.

The Si/Al ratio in a series of H-ZSM-5 catalysts (H-ZSM-5 Si/Al=25, 40 and 140) was changed to assess the influence of acid site density (Table 4). Although formaldehyde conversion (in the 44-50% range) is relatively constant, selectivity clearly changes with the Si/Al ratio. Prins condensation products (**I** and **IV**) dominate the product distribution with a combined selectivity of 82%-90%, over all H-ZSM-5 catalysts. Although **III** and **V** formed, these reaction pathways do not contribute significantly and for the most part are unaffected by the Si/Al ratio. At the lowest and highest Si/Al ratios (25 and 140), **I** is the predominant product and **IV** the second five-carbon product. At Si/Al=40, **I** dehydrates faster, leading to **IV** selectivity of about 55% at about 44% formaldehyde conversion (**IV** yield of 22% based on initial formaldehyde). This yield is higher than that obtained from traditional cracking processes.³⁶ Notably, this is the only successful example of selective one-step formation of **IV** at such low temperatures (423K). The one-step, gas-phase formaldehyde-isobutene condensation to **IV** usually requires temperatures higher than 573K and coking appears to be the main drawback under these conditions.¹²

To investigate the effect of Si/Al ratio on the dehydration step, we carried experiments with **I** over H-ZSM-5 with varying Si/Al ratios (Table 5). A control experiment with no catalyst showed no dehydration of **I** under the present conditions. Over H-ZSM-5(25) and H-ZSM-5(40), **I** converted fully and **IV** formed selectively. On the other hand, over H-ZSM-5(140), **I** conversion was incomplete because the density of acid sites decreases with the Si/Al ratio, but **IV** was still the predominant product. Compound **V** formed because reverse Prins reaction yields formaldehyde and isobutene and thereby **V** can form either by Prins cyclization (**I** reaction with formaldehyde) or by Hetero-Diels-Alder of **IV** with formaldehyde. **III** was not detected, suggesting that this molecule forms via a direct parallel reaction of excess formaldehyde with isobutene. These experiments explain why H-ZSM-5(40) is an efficient catalyst for the one-step **IV** formation, whereas H-ZSM-5(140) does not favor dehydration of **I**. Starting from formaldehyde and isobutene (Table 4, compare entries 4 and 5) over adjusted amount of H-ZSM-5(40), so as to have the same number of acid sites (H+) as in H-ZSM-5(140), demonstrates that the acid site density does not affect the Prins reaction step in terms of product distribution. However, under the present experimental conditions, higher catalyst amount is required for the second dehydration step of **I** to proceed in a tandem manner.

Thermogravimetric analysis of the spent catalysts (Figure 1A and B) was used to quantify the formation of large byproducts in the catalyst pores. The weight loss of the spent samples is higher for the catalyst with Si/Al=25, followed by Si/Al=40 and 140, but it is in all cases near 15%. This is close to the pore volume of the ZSM-5 samples (assuming a density of $\sim 1 \text{ g cm}^{-3}$). There are three stages of weight loss, as revealed by the differential analysis (Figure 1B). A large low-temperature peak ($\sim 420 \text{ K}$), a smaller intermediate peak ($\sim 550 \text{ K}$) and there is a high temperature peak at about 800K, with a magnitude that follows the same trend (Si/Al=25 > Si/Al=40 > Si/Al=140). Because of the larger peak at high temperatures, catalyst deactivation/active site and pore blocking seems more significant for the samples with lower Si/Al ratios.

Table 4 Conversion and selectivity for the isobutene and formaldehyde reaction. T=423K, $t_r=1\text{h}$, $\text{C}_4\text{H}_8/\text{CH}_2\text{O}$ molar ratio=3.15, catalyst amount=0.25g, TON was calculated based on the sum of product moles and the number of acid sites,^a Same number of acid sites (H+) as entry 5, adjusted by varying catalyst amount

Catalyst	CH ₂ O	TON	Carbon-based Selectivity (%)
----------	-------------------	-----	------------------------------

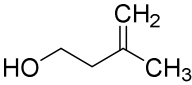
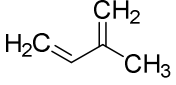
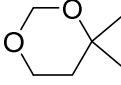
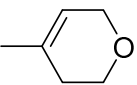
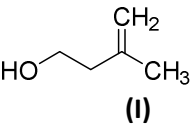
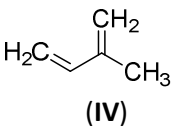
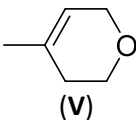
	Conversion (%)					
None	-	-	-	-	-	-
H-ZSM-5(25)	43.8	8.3	79.7	7.8	4.1	8.5
H-ZSM-5(40)	44.3	12.8	27.3	54.5	3.6	13.6
H-ZSM-5(40) ^a	42.8	44.7	85.9	3.3	2.5	4.2
H-ZSM-5(140)	49.6	53.0	84.4	5.6	1.6	5.3
H-beta(19)	18.0	1.9	0.0	44.1	0.0	55.9

Table 5 Effect of Si/Al ratio on 3-methyl-3-buten-1-ol reactivity. T=423K, t_r=1h, catalyst/C₅H₁₀O wt=3.7

Catalyst	Conversion (%) 	Carbon-based Selectivity (%)	
			
None	-	-	-
H-ZSM-5(25)	99.3	94.9	5.1
H-ZSM-5(40)	100.0	94.0	6.0
H-ZSM-5(140)	59.0	89.8	10.2

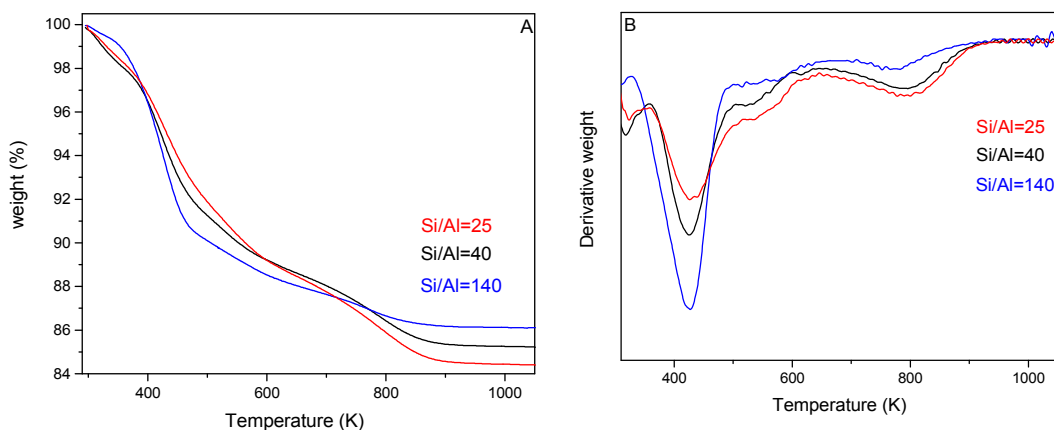


Figure 1 Actual (A) and derivative weight (B) versus temperature for spent samples with different Si/Al ratios, Analysis conditions: air flow=50ml/min, rate=10°/min, temperature=room temperature to 1100K, Reaction conditions: Temperature=423K, $t_r=1$ h, C_4H_8/CH_2O molar ratio=3.15, catalyst amount=0.25

In summary, under the reaction conditions investigated here, H-ZSM-5 catalyzes the formation of 3-methyl-3-buten-1-ol (**I**)—the desired isoprene precursor. When water is used as solvent, the formaldehyde conversion decreased from 44.3% to only 0.8%. This is probably due to the low solubility of isobutene in water, but it is also possible that water adsorbs stronger than formaldehyde poisoning the zeolite acid sites. The Si/Al ratio affects the dehydration rate of **I** and the rate of side reactions; Si/Al=40 shows an excellent balance between reaction rate and selectivity for the one-step isoprene formation at 423K.

3.3 Reaction network

We monitored the reaction with time using H-ZSM-5(40) at 423K to quantify the evolution of the product distribution (Figure 2). We also investigated the reaction evolution at 323 and 348K (see Figures S3 and S4). Species **I** is the predominant product at short reaction times (0.5h) but its yield decreases as the reaction progresses, while the yield of isoprene (**IV**) increases in parallel. It then follows that as **I** accumulates, the dehydration rate to **IV** increases: **I** is the only **IV** precursor observed under these experimental conditions. Species **III** forms at very low yields and is a final stable compound. Finally, the yield of **V** increases slightly with time, suggesting that the rate of this reaction increases slowly and that **V** is not consumed in another reaction.

We explored the reaction network using the reaction intermediates and products as reactants in a series of experiments over H-ZSM-5(40), at 423K (Table 6).

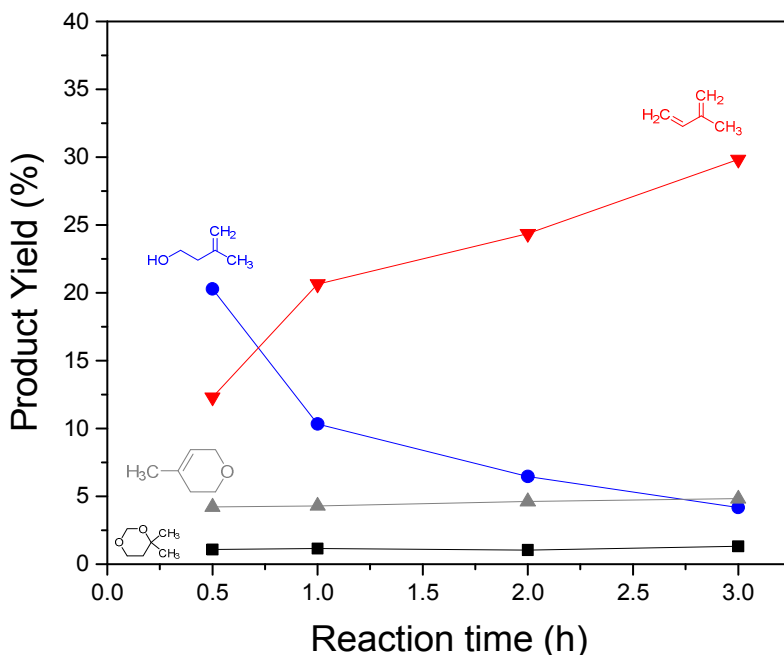
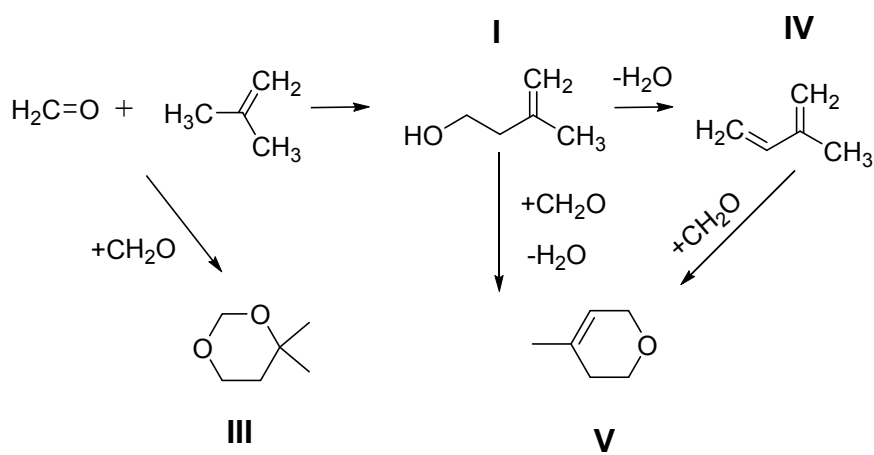


Figure 2 Product Yield versus reaction time. Catalyst: H-ZSM-5(40), T=423K, C₄H₈/CH₂O molar ratio=3.15, catalyst amount=0.25g

Table 6 Reactivity of reaction intermediates and products. Catalyst: H-ZSM-5(40), T=423K, t_r=1h, CH₂O/C₅H₁₀O or C₅H₈ molar ratio=4.2, catalyst amount=0.25gr

Reactants	CH ₂ O Conversion (%)	I/IV Conversion (%)	Carbon-based Selectivity (%)	
			$\text{H}_2\text{C}=\text{CH}-\text{C}(\text{CH}_3)=\text{CH}_2$ (IV)	 (V)
I & CH ₂ O	10.4	100.0	8.4	91.6
IV & CH ₂ O	5.3	80.0	-	100.0

Compound **I** reacts to completion with formaldehyde (in excess) and forming **V** in high selectivity (91.6%). **IV** was the secondary product with 8.4% selectivity. When formaldehyde is in excess, **I** undergoes Prins cyclization rather than dehydration to **IV**. A second reaction that also leads to the formation of **V** is Hetero-Diels-Alder of **IV** with formaldehyde, as evidenced by an experiment using these two as reactants. The above experiments in combination with the time-dependent yield profiles lead to the reaction network shown in Scheme 2.



Scheme 2 Reaction network of formaldehyde reaction with isobutene

3.4 Reaction parameters

C_4H_8/CH_2O molar ratio.

Increasing the molar ratio from 1.6 to 3.15 (Figure 3) increases the formaldehyde conversion from 13.5 to 44.3%, while further increasing the ratio to 6.3 has a less pronounced effect on formaldehyde conversion (44.3 versus 52.9%). Isobutene and formaldehyde, both Lewis bases, compete for the same Bronsted acid sites.¹⁶ Both **I** and **IV** yields are favored by higher C_4H_8/CH_2O molar ratios but the effect is not marked when we increased the ratio to 6.30. A ratio of 3.15 is thus preferred to reduce the amount of excess isobutene. An observed side reaction is isobutene hydration to t-butanol. The extent of isobutene hydration increases with the C_4H_8/CH_2O ratio and with the promotion of water-forming side reactions, such as dehydration of **I** to **IV** and paraformaldehyde decomposition to formaldehyde. Note that a C_4H_8/CH_2O ratio of 3.15 is lower

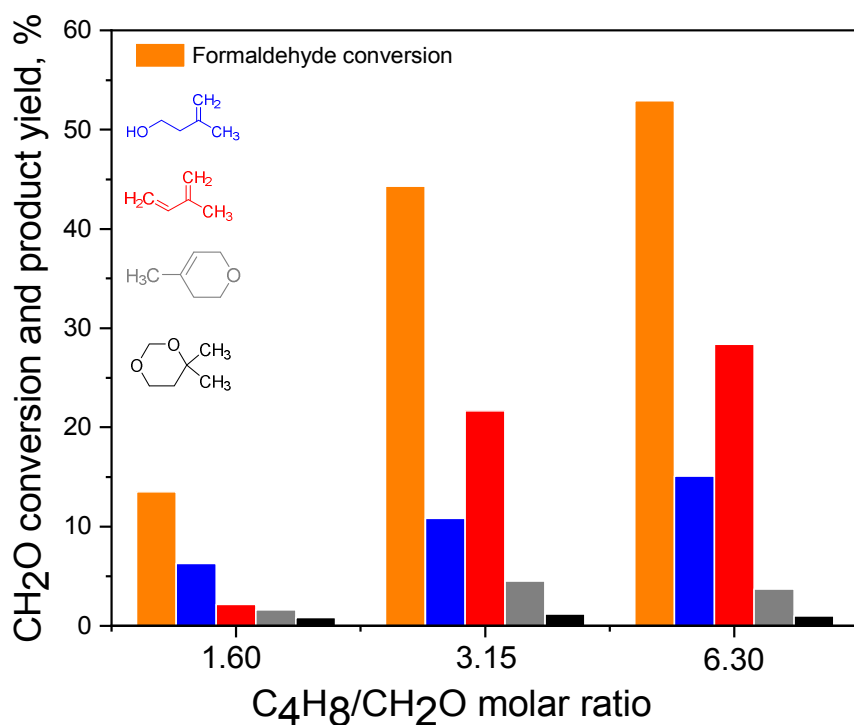


Figure 3 Effect of C_4H_8/CH_2O molar ratio on product yield. Catalyst: H-ZSM-5(40), $T=423K$, $t_r=1h$, catalyst amount=0.25g

than those used in recent literature, where ratios up to 17 have been used.³⁷

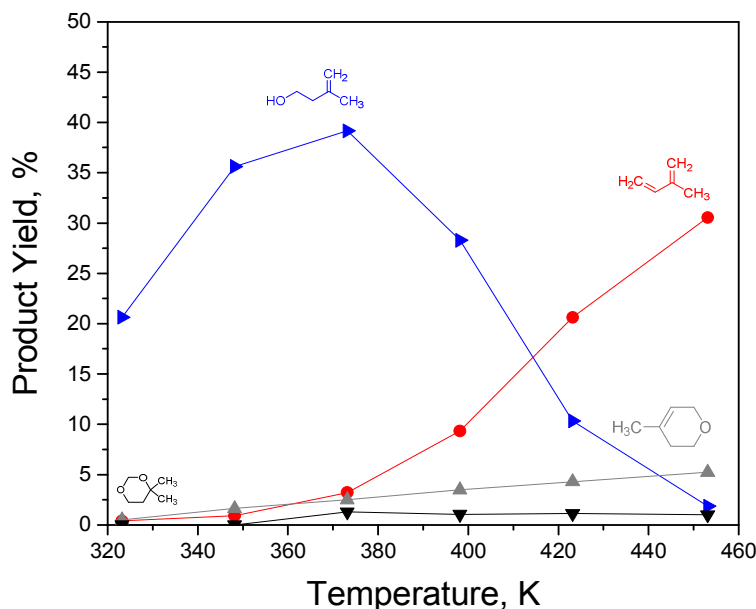


Figure 4 Effect of reaction temperature on product yield. Catalyst: H-ZSM-5(40), $t_r=1h$, C_4H_8/CH_2O molar ratio=3.15, catalyst amount=0.25gr

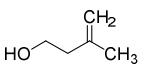
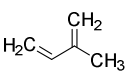
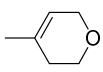
Reaction temperature. Temperature has a significant effect on the dehydration rate of **I**, but only a minor effect on the yield of six-carbon products. Only the yield of **V** increases slightly with temperature, which could be due to increased concentration of **IV** and to the Hetero-Diels-Alder reaction with formaldehyde becoming more important at higher temperatures (Scheme 2). At low temperatures, **I** is the primary product; at a temperature as low as 323K, about 20% **I** yield is obtained (selectivity is about 91%, Table S2). 3-methyl-3-buten-1-ol (**I**) yield increases with temperature up to 373K and then decreases as dehydration rate to **IV** increases. At temperatures higher than about 415K, **IV** becomes the primary product. At higher temperatures oligomerization reactions are also catalyzed decreasing the extent of Prins condensation. This can be seen from CH_2O conversion data presented in Table S2. The TGA of the spent samples after reaction at 373 and 423K (Figure S5) clearly show that higher temperatures favor undesired reactions. Notably, one-step **IV** production has only been achieved in vapor-phase at temperatures higher than 513K.¹⁵

CH_2O /catalyst ratio. We increased the amounts of formaldehyde and isobutene (at a fixed molar ratio) and fixed amount of catalyst of 0.25g (Table 7). The first entry corresponds to a CH_2O /catalyst ratio of 0.4. Formaldehyde conversion does not change appreciably; it ranges between 44% and 55%

in all cases. On the other hand, turn over number (TON) and catalyst productivity to the Prins condensation increase almost linearly with CH₂O/catalyst ratio; that is, H-ZSM-5(40) is highly active for Prins reaction. Product selectivity shows a clear trend with varying CH₂O/catalyst ratio: selectivity to 3-methyl-3-buten-1-ol (**I**) decreases with the ratio whereas that of **IV** mirrors the opposite trend as required by stoichiometry. Selective one-step **IV** formation is achieved only at CH₂O/catalyst ratio=0.4, while **I** is the primary product at any other ratio; selectivity up to 86.0% is obtained at high ratios. It seems that the rate of dehydration of **I** is limited as reactant amounts increase. The latter is also evident from t-butanol yield; water available for isobutene hydration to t-butanol primarily forms from **I** dehydration to **IV** and, since water concentration decreases as the ratio increases, the former reaction decreases as well. Selectivity to **V** decreases because of the lower concentrations of isoprene at low catalyst amounts; this is consistent with **V** formed by the Hetero-Diels-Alder of **IV** with formaldehyde.

We used the amount of **I** produced from the experiment with a CH₂O/catalyst ratio wt=4.0 (Table 7 entry 5) and performed a second dehydration step under the same experimental conditions. **I** dehydrates at 69.0% conversion and isoprene selectivity is higher than 93.0% resulting in a catalyst productivity to isoprene of $1.6 \text{ gr}_{\text{prod}} \cdot \text{gr}_{\text{cat}}^{-1} \cdot \text{h}^{-1}$. This suggests that under the highest catalyst productivity conditions, a two-step isoprene process is preferred. In addition, our experiments on the effect of temperature on the second dehydration step indicate that 423K is a suitable temperature to run the reaction (see Table S3).

Table 7 Effect of CH₂O/catalyst ratio. Catalyst: H-ZSM-5(40), T=423K, t_r=1h, catalyst amount=0.25gr, catalyst productivity is calculated as the sum of Prins condensation products (**I** and **IV**) per catalyst amount and t_r, TON was calculated based on the sum of product moles and the number of acid sites

CH ₂ O/catalyst ratio wt	CH ₂ O Conversion, %	TON	Catalyst productivity, $\text{gr}_{\text{prod}} \cdot \text{gr}_{\text{cat}}^{-1} \cdot \text{h}^{-1}$	 (I)	 (IV)	 (III)	 (V)	t-butanol Yield (%)
0.4	44.3	12.8	0.32	27.3	54.5	3.6	13.6	13.90
0.8	48.8	29.8	0.90	77.2	11.3	4.4	5.5	8.40
1.2	54.7	50.4	1.56	83.2	5.9	3.8	5.2	1.94

2.0	49.5	76.5	2.37	86.0	2.5	4.8	3.6	0.91
4.0	52.6	163.6	4.96	85.8	0.8	5.3	2.2	0.70

3.5 Reactivity of butene isomers

Formaldehyde was reacted with isobutene, 1-butene and cis-2-butene, to study differences in reactivity and product selectivity (Table 8). The order of reactivity observed is: isobutene > 1-butene > cis-2-butene. This is in agreement with theoretical calculations (*see below*) and previous findings in the thermal ene reaction of butenes with diethyl azodicarboxylate.³⁸ For isobutene, the major product is the unsaturated alcohol **I** and its dehydration product isoprene (**IV**), while a different unsaturated alcohol isomer **VI** is only formed in a small quantity. Our calculations found (*see below*) that **VI** formation has a higher free energy of activation than formation of **I** (9.1 vs. 5.7 kcal/mol). 1-butene forms two 3-penten-1-ol isomers, while cis-2-butene results in a mixture of unsaturated five-carbon alcohol isomers, (2-methyl-3-buten-1-ol is the main product), plus six-carbon products **III** and **V**.

Table 8 Reactivity and formed products of Prins condensation of formaldehyde with butene isomers. T=423K, $t_r=1h$, C_4H_8/CH_2O molar ratio=3.15, H-ZSM-5(40), catalyst amount=0.25g

Olefin	Rate relative to isobutene	Products detected (selectivity, %)
Isobutene	1.0	I (27.3%), VI (1.1%), IV (54.5%), III (3.6%), V (13.6%)
1-butene	0.15	VII (68.6%), VIII (31.4%)
Cis-2-butene	0.13	I (3.9%), III (18.7%), V (51.5%), VII (7.3%), VIII (5.0%) IX (13.5%),

3.6 Prins condensation reaction mechanism over Brønsted acids

According to electronic structure calculations and experimental support, the thermal carbonyl-ene reaction follows a concerted mechanism through a single, rather asynchronous transition state complex with a six-membered ring geometry. The reaction is quite slow, with activation energy of *ca.* 36 kcal/mol or higher, but it can be catalyzed by Lewis acids via coordination of the enophile and an electronic

mechanism readily understood in terms of frontier molecular orbital theory—the Lewis acid lowers the LUMO of the enophile and closes the energy gap to the HOMO of the ene.³⁹ Over Lewis acids, the single transition state retains its six-membered ring geometry but becomes more zwitterionic in character and substantially more asynchronous owing to development of negative charge on the carbonyl oxygen atom and the electrostatic repulsion between it and the π -electrons of the ene.⁴⁰ Overall, the mechanism of the reaction over Lewis acids is well understood, elucidated by quantum chemical calculations in the gas phase with typical Lewis acids (e.g., AlCl_3 , SnCl_4 etc.), in ion-exchanged zeolites (e.g., Cu(I)-Y , Ag(I)-Y and Au(I)-Y) and metalorganic frameworks (e.g., MOF-11 with Cu(II) active site).⁴¹⁻⁴⁷ Similarities between the carbonyl-ene reaction and the (hetero) Diels-Alder reaction have also been pointed out and analyzed. In addition, the mechanism of C-C coupling between formaldehyde and other substrates such as dihydroxyacetone over framework lewis acidic Sn sites in Sn-Beta has been studied experimentally.⁴⁸

The mechanism over Brønsted acids is not as well studied. Here we investigate the Prins reaction of three isomers of butene (2-methyl-propene (isobutene), 1-butene and cis-2-butene) over H-ZSM5 zeolite using quantum chemical calculations. We have not been able to find a single-transition-state mechanism for the Brønsted-catalyzed reaction, but rather a two-step one that formally entails protonation of the formyl group, electrophilic attack on the alkenyl group and deprotonation of the resulting intermediate carbocation (Scheme 1, pathway to product I). Zero-point corrected energy profiles are shown in Figure 5; free energy profiles at 150 °C are shown in Figure 7, below, and are discussed separately later in the text.

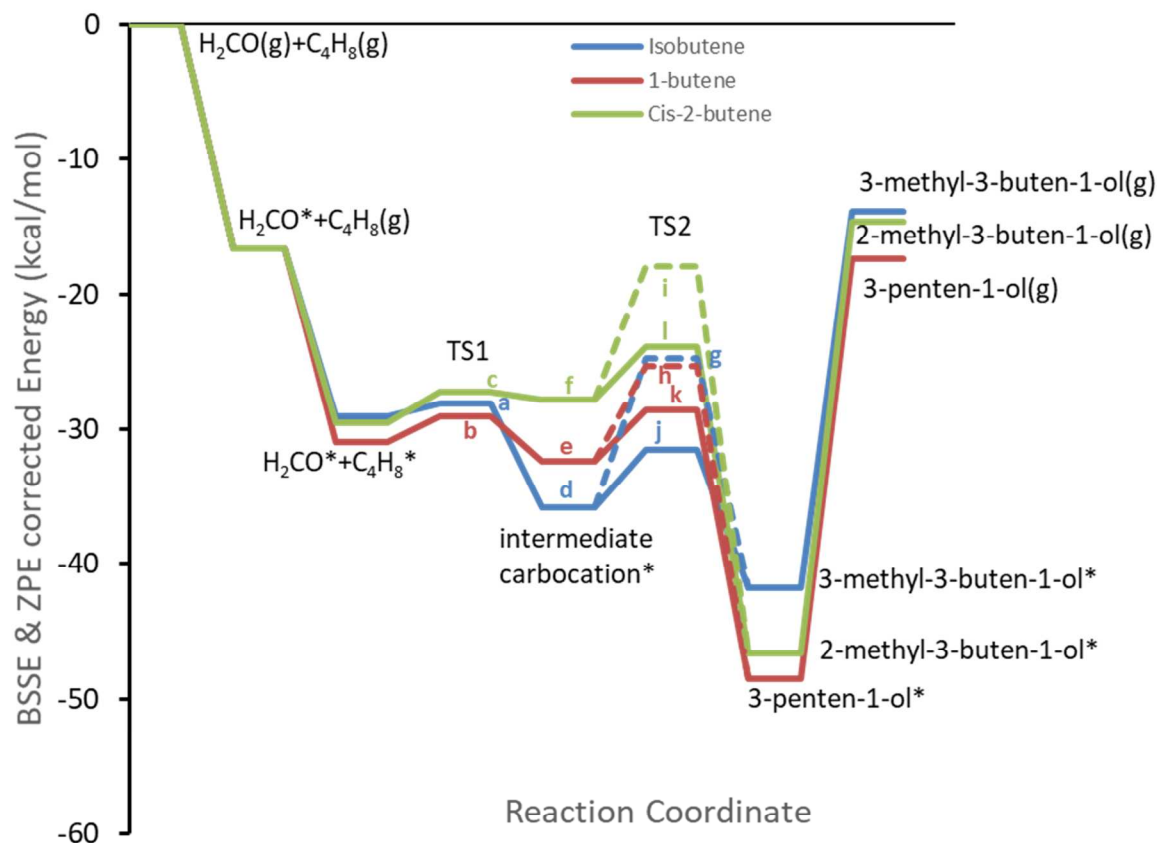


Figure 5. Zero-point corrected energy profiles for the Prins reaction of formaldehyde (H_2CO) with three isomers of butene over H-ZSM5: isobutene (blue), 1-butene (red) and cis-2-butene (green); '*' signifies adsorbed species. TS1, transition state of electrophilic attack; TS2, transition state of deprotonation of intermediate and catalyst regeneration. In the case of cis-2-butene, electrophilic attack occurs in TS2. Dashed lines, pathway for direct deprotonation of the allylic carbon (see text for details); solid lines, pathway for deprotonation of the intermediate via OH-mediated H-shuffling mechanism and six-membered ring transition state geometry (see text for details). State labels correspond to structures shown in Figure 6.

In the co-adsorbed state of the ene-enophile interacting complex, we see preferential coordination of formaldehyde to the Al-OH-Si bridge via hydrogen bonding. Despite isobutene having higher proton affinity than formaldehyde, by ca. 21.4 kcal/mol, our calculations show that formaldehyde binds more strongly to the acid site by ca. 2.5 kcal/mol. In this most favorable geometry of the interacting complex, the C=O bond of formaldehyde is slightly elongated by 0.02 Å and the Al-bridge proton is partially delocalized (OH elongation by 0.05 Å). Digressing briefly to consider that paraformaldehyde was used as the source of formaldehyde, it would be reasonable to expect that initially the active sites would be occupied by some oligomer of oxymethylene (which readily depolymerizes in the presence of a Brønsted proton) or by formaldehyde monomers at a 2:1 ratio (or higher) from depolymerized oligomer. We have

thus also investigated the binding of the dimer of formaldehyde ($\text{HO-CH}_2\text{-O-CH}_2\text{-H}$) and of two formaldehyde monomers to the active site and found that the respective binding enthalpies are 40.8 and 27.4 kcal/mol, further confirming that none of the alkenes considered in this study would compete with the formaldehyde molecule for coordination to the active site.

Returning to the main thread, the co-adsorbed ene-enophile complex requires very modest activation to reach the first transition state for electrophilic attack: *intrinsic* energy barriers of 0.95, 1.94 and 2.25 kcal/mol for isobutene, 1-butene and cis-2-butene, respectively. Geometries of this transition state are shown in Figure 6 (a)-(c) for isobutene and the other two isomers. We argue that these energy barriers are not determined by the relative stabilities of the resulting intermediate carbocations but rather by the nucleophilic character of the carbon atom being attacked. This explains why the barrier for 1-butene is somewhat lower than that for cis-2-butene even though both lead to 2° carbocations, the error inherent in quantum chemical computations notwithstanding. To appreciate this, we need to look into the structure and nature of the first transition state more closely.

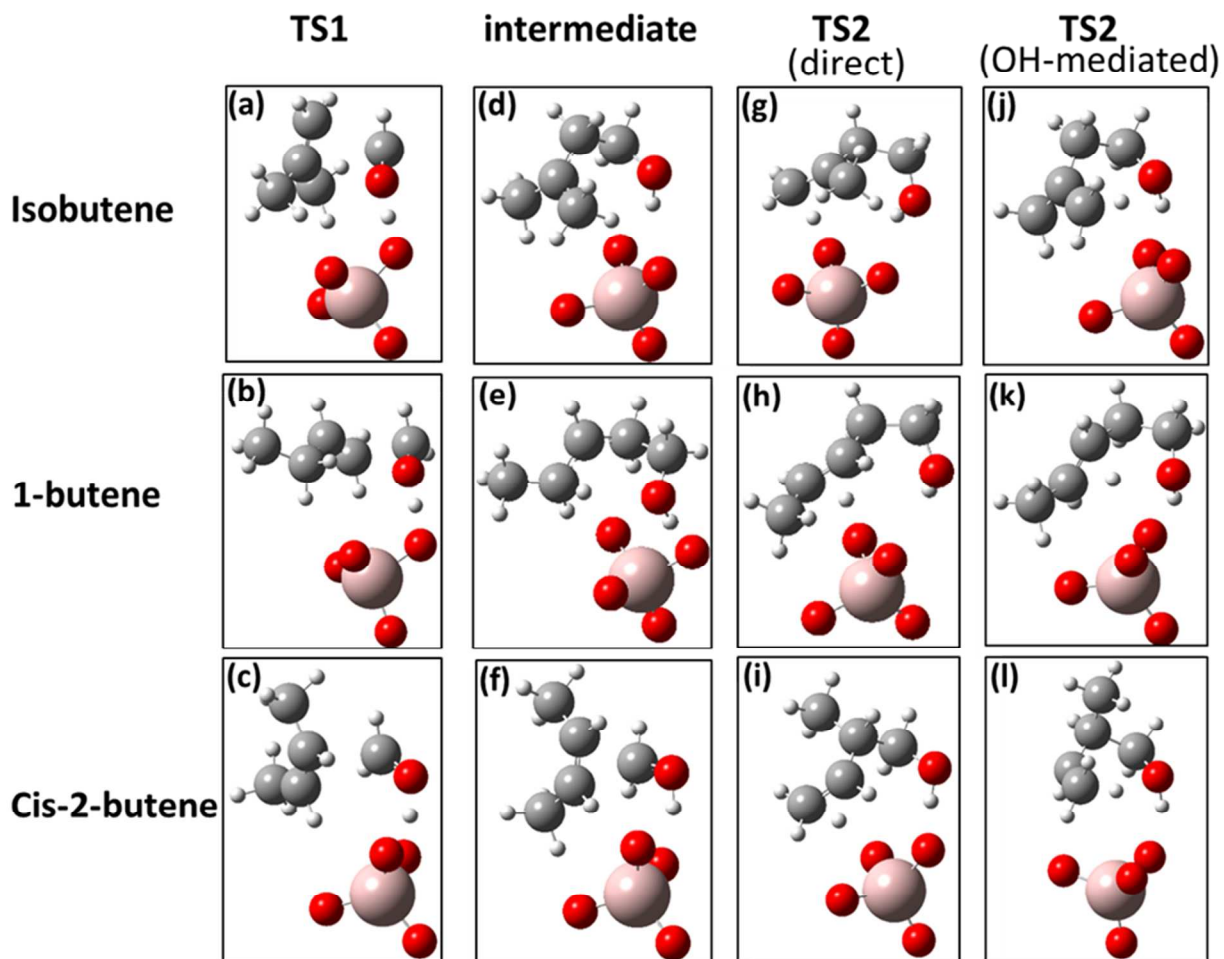


Figure 6. Transition states and intermediate geometries correspond to the energy profile in Figure 5 and 7. Color codes: Pink, Al; red, O; gray, C; and white, H. For clarity we only show the structure of the active site.

In the first transition state, the acidic proton is completely delocalized, half-way between the donor and acceptor O atoms, and the carbonyl carbon electrophilically attacks the double bond of the ene (Figure 6, (a)-(c)). Despite the proton delocalization, the length of the forming $\sigma(C - C)$ bond (2.46, 2.35 and 2.54 Å for isobutene, 1-butene and cis-2-butene respectively), and the absence of the corresponding $\sigma(C - C)$ orbital in the NBO analysis indicate that this is an early, reactant-like transition state. By comparison, in the concerted transition state over Lewis acids (also see Figure S7), the C-C bond is more developed; for example, it is about 1.6 Å long for propene and formaldehyde coordinated to AlCl_3 (computed in the gas phase at the B3LYP/6-31G* theory level).⁴⁰ Besides proton delocalization, the population of formaldehyde's LUMO ($\pi^*(C - O)$) population of 0.14 electrons), the depopulation of

isobutene's HOMO ($\pi(C - C)$ population of 1.8 electrons) and the substantial second-order perturbation theory mixing of the two orbitals summarize the most salient electronic features of the first transition state. In this state, the NBO analysis does not show development of the $\pi(C - C)$ bond of the product either. Thereby, the reactant-like transition state suggests that the stability of the ensuing carbocation, *which is not yet formed*, should not be a factor in the energetics of the first step—the latter should primarily be determined by the nucleophilic character of (equivalently, negative charge localization on) the ene carbon being attacked; that is the C1 (methylene group) carbon of isobutene (2-methyl-propene), the C1 (methylene) carbon of 1-butene and the C2 (methine group) carbon of cis-2-butene. On account of resonance (valence bond structures contributing to the ground electronic state), the degree of electron density localization on the nucleophilic carbon depends on the substituents of the carbon atom to which it is double-bonded, namely, the C2 carbon in isobutene, the C2 in 1-butene and the C3 in cis-2-butene. In isobutene, the C2 carbon has two electron donating substituents, whereas the C2 and C3 of 1-butene and 2-butene, respectively, are singly substituted. Indeed, from the charge distributions shown in Figure S6 of the SI section, the charges on the carbon atoms being attacked by the protonated formyl group are -0.582, -0.410 and -0.2e for isobutene, 1-butene and 2-butene, respectively, indicating the decreasing nucleophilic character. The reason behind 2-butene's decreased nucleophilicity (relative to 1-butene) is quite simply the symmetry of its electronic wave function, as a result of which the charge on the 2-butene carbon is half that on 1-butene. This depletion in charge distribution on the alkenyl carbons of 2-butene is in fact so substantial that we do not find an intermediate carbocation past the first transition state. The structures of the intermediates for the three isomers are shown in Figure 6 (d)-(f). Unlike isobutene and 1-butene, for which the electrophilic addition proceeds to completion and yields intermediate 3° and 2° carbocations, cis-2-butene only forms a complex with the protonated formaldehyde (see Figure 6 (f))—the corresponding, fully formed 2° carbocation (not shown) is higher in energy by *ca.* 6 kcal/mol. This also explains why this step is exoergic for isobutene, less so for 1-butene and endoergic for cis-2-butene. (There is an interesting, fine point to be made here, that although formaldehyde by itself is not basic enough to accept the acidic proton, cis-2-butene acts as a stabilizing agent of the protonated adduct. This suggests that the (cis-2-butene)-formaldehyde complex is held together by more than van der Waals forces.)

The second transition state involves proton loss and concomitant double bond formation at the allylic position of the ene; for cis-2-butene, it also involves simultaneous formation of the ene-enophile $\sigma(C - C)$ bond. We have identified two distinct hydrogen elimination pathways: one involves direct proton back-donation from the allylic carbon to the active site (Figure 6, (g)-(i)); and the other hydroxyl-

mediated proton shuffling, whereby the allylic carbon donates a proton to the oxygen of the hydroxyl group (1,5 H-shift) which in turn donates its own proton back to the active site (Figure 6, (j)-(l)). In the latter case, the transition state assumes a six-membered ring geometry reminiscent of the concerted mechanism followed by the thermal and Lewis acid-catalyzed reactions. Remarkably, the proton shuffling transition state is energetically favored.

In the direct deprotonation pathway, the corresponding intrinsic energy barriers are *ca.* 11, 7 and 9.4 kcal/mol for isobutene, 1-butene and *cis*-2-butene, respectively, and the associated transition states are the highest-lying ones along the entire pathway; we shall return to kinetics related aspects when we discuss the free energy profiles. For all three isomers, the transition state is characterized by a delocalized allylic proton (Figure 6 (g)-(i)) with partial charges ranging between 0.44 and 0.49*e*. The fractional charges are consistent with the Mulliken charge transfer picture—and indeed our current understanding—of proton transfer, according to which proton transfer is activated by electron density shift from a lone pair of the acceptor atom to the donor-H antibonding orbital.⁴⁹ Within this framework, we can readily rationalize the relative intrinsic barriers for isobutene and 1-butene, for which the $\sigma^*(C-H)$ orbital energies are 0.392 and 0.330 Hartree, respectively, and correlate with the computed energy barriers; the lower the energy of the $\sigma^*(C-H)$, the stronger the electronic coupling to the lone pair of the acceptor and thus the more facile the proton transfer. (In principle, one should be comparing the energy gap, $\Delta E_{n \rightarrow \sigma^*}$, between the $\sigma^*(C-H)$ of the proton donor and the non-bonding, lone pair of the proton acceptor. In the direct mechanism, however, the proton acceptor is common to both substrates—the oxygen atom of the active site.) In the case of *cis*-2-butene, the allylic proton loss does not readily comport with this framework. Indeed, the $\sigma^*(C-H)$ orbital energy of the breaking bond in the ene-enophile complex is 0.424 Hartree, predicting a proton loss barrier higher than that for isobutene—it is actually *lower* by about 1.6 kcal/mol. The reason is that, as we noted earlier, the electrophilic addition does not afford a carbocation and the second step of the reaction entails $\sigma(C-C)$ bond formation in addition to allylic proton loss.

For the hydroxyl-mediated deprotonation involving the six-membered ring transition state and proton shuffling, the corresponding intrinsic barriers are 4.3, 3.8 and 3.5 kcal/mol for isobutene, 1-butene and *cis*-2-butene, respectively; a significantly faster pathway. Geometries of these transition states are shown in Figure 6 (j)-(l). For isobutene, and unlike the direct deprotonation pathway, this transition state lies *lower* than that for the electrophilic addition. For the other two isomers, this transition state lies higher than the electrophilic addition one, as in the direct mechanism. Using the $\sigma^*(C-H)$ and $n(O)$ NBO energies, where $n(O)$ denotes the lone pair of the hydroxyl oxygen accepting the allylic

proton, the descriptor $\Delta E_{n \rightarrow \sigma^*}$ takes on the values of 0.812, 0.748 and 1.189 Hartree, for isobutene, 1-butene and cis-2-butene, respectively. We see again that the smaller $\Delta E_{n \rightarrow \sigma^*}$ gap correlates with the lower barrier for the two isomers that give carbocations upon electrophilic addition.

In Figure 7, we show the free energy profiles for all the Prins pathways examined. For all three butene isomers, the dominant pathway is the one that goes through the hydroxyl mediated hydrogen elimination transition state with a six-membered ring geometry. The rate-limiting step, however, is not the same for all three isomers; for isobutene, it is the electrophilic attack, whereas for the other two it is the hydrogen elimination. The relative positions of the transition states are the same on the free energy scale as on the zero-point corrected energy scale, suggesting that the rate-limiting step is primarily determined by electronic phenomena and not by entropic contributions. According to the energy span model,⁵⁰⁻⁵² the turnover frequency determining apparent activation energy of the Prins reaction is given by the energy span between the second transition state and the most stable, preceding intermediate—in this case one of the two intermediate states prior to the first transition state. For isobutene, 1-butene and cis-2-butene the free energy spans are 5.7, 8.8 and 12.9 kcal/mol, respectively, at 150 °C. The predicted relative reactivities for the Prins reaction correlate with the relative reaction rates presented in Table 8. We should remind the reader, however, that the relative reactivity figures of Table 8 refer to the overall reaction, inferred from the conversion of formaldehyde after 1 hour of reaction. Based on our calculations and the experimental data using different butene isomers, isobutene is the most reactive one and also follows desired pathways leading to the formation of the unsaturated alcohol **I** and the desired diene, **IV**.

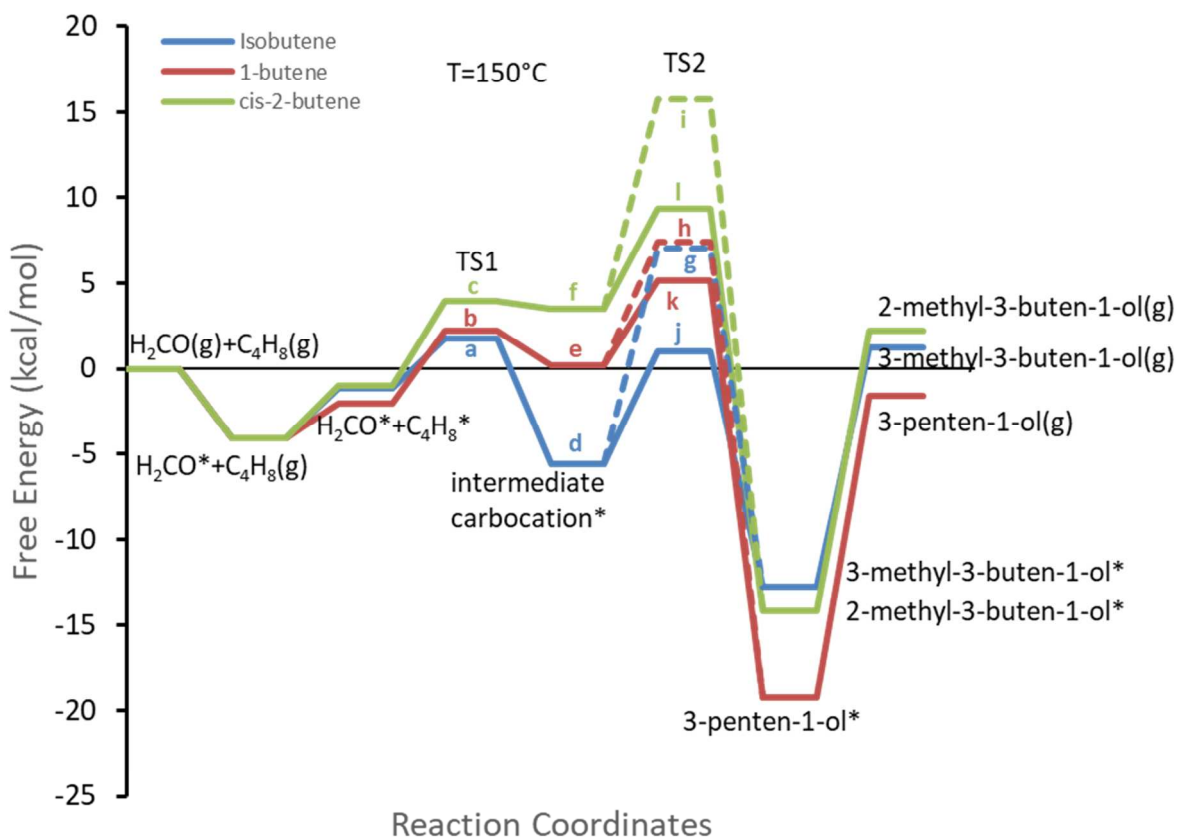


Figure 7. Free energy profiles for the Prins reaction of formaldehyde (H_2CO) with three isomers of butene over H-ZSM5: isobutene (blue), 1-butene (red) and cis-2-butene (green; ‘*’ signifies adsorbed species). TS1, transition state of electrophilic attack; TS2, transition state of deprotonation of intermediate and catalyst regeneration. In the case of cis-2-butene, electrophilic attack occurs in TS2. Dashed lines, pathway for direct deprotonation of the allylic carbon (see text for details); solid lines, pathway for deprotonation of the intermediate via H-shuffling mechanism and six-membered ring transition state geometry (see text for details). Energies are referenced to isolated reactants. State labels correspond to structures shown in Figure 6.

4. Conclusions

H-ZSM-5 zeolites with different Si/Al ration are shown to catalyze the Prins condensation between formaldehyde and different butene isomers. The reactions are catalyzed with selectivity to 3-methyl-3-buten-1-ol (I) or isoprene (IV) depending on reaction conditions. We have used quantum chemical calculations to understand the different reactivity of butene isomers and found that a critical factor that determines reactivity is the nucleophilicity of the alkene carbon atom being attacked. The mechanistic steps for this reaction include protonation of formaldehyde, electrophilic attack on the alkene and deprotonation of the resulting intermediate carbocation. For isobutene and 1-butene we found that the electrophilic addition occurs simultaneously upon protonation of the formyl group, but for cis-2-butene

it is coordinated with the proton back-donation step. The calculations also showed a switch in the rate-determining step: from electrophilic addition for isobutene to hydrogen elimination for 1-butene and cis-2-butene. H-ZSM-5 was identified as the most effective and selective for formation of 3-methyl-3-buten-1-ol from condensation between formaldehyde and isobutene; sequential undesired Prins cyclization and hetero-Diels-Alder reactions are limited. Finally, isoprene forms under optimal reaction conditions either in a second dehydration step or in a single-step over H-ZSM-5 with optimal acid site density.

Conflicts of interest

There are no conflicts to declare

Acknowledgments

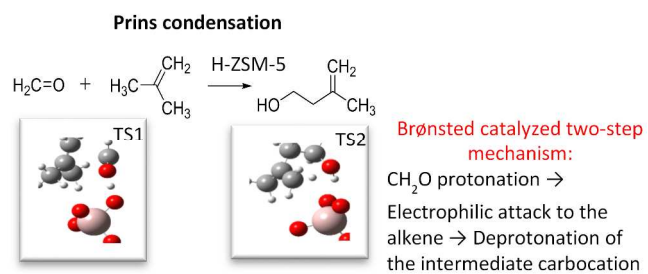
Research was supported as part of the Catalysis Center for Energy Innovation, an Energy Frontier Research Center funded by the U.S. Department of Energy (DOE), Office of Science, Basic Energy Sciences (BES), under Award number DE-SC0001004

References

- 1 K. W. George, M. G. Thompson, A. Kang, E. Baidoo, G. Wang, L. J. G. Chan, P. D. Adams, C. J. Petzold, J. D. Keasling and T. Soon Lee, *Sci. Rep.*, 2015, **5**, 1–12.
- 2 J. van S. A Hull, I Golubkov, B Kronberg, T Marandzheva, *Int. J. Engine Res.*, 2006, **7**, 203–214.
- 3 J. H. Mack, V. H. Rapp, M. Broeckelmann, T. S. Lee and R. W. Dibble, *Fuel*, 2014, **117**, 939–943.
- 4 <http://www.kuraray.eu/en/produkte/product-ranges/isoprenol/>. (Accessed January, 2018)
- 5 T. A. M. G.O. Ezinkwo, V.F. Tretjakov, R.M. Talyshinky and A.M. Ilolov, *Catalysis for sustainable energy*, 2013, 100–111.
- 6 V. L. Sushkevich, V. V Ordonsky and I. I. Ivanova, *Applied Catal. A, Gen.* 2012, **441–442**, 21–29.
- 7 A. Krzywicki, T. Wilanowicz and St.Malinowski, *React. Kinet. Catal. Lett.*, 1979, **11 (4)**, 399–403.
- 8 M. Yanagita and T. Mitsui, U.S. Patent 3,253,051, 1966.
- 9 M. Ai, *J. Catal.* 1987, **106**, 280–286.
- 10 E. Dumitriu, V. Hulea, I. Fechete and C. Catrinescu, *Applied Catal. A, Gen.* 1999, **181**, 15–28
- 11 E. Dumitriu, D. T. On and S. Kaliaguine, *J. Catal.* 1997, **160**, 150–160.
- 12 Zh. Dang, J. Gu, L. Yu and Ch. Zhang, *React. Kinet. Catal. Lett.* 1991, **43 (2)**, 495–500.

- 13 O. S. Pavlov, S. A. Karsakov and S. Y. Pavlov, *Theoretical Foundations of Chemical Engineering* 2011, **45 (4)**, 487–491.
- 14 M. Shamzhy, M. Opanasenko, O. Shrets and J. Cejka, *Front. Chem.* 2013, **1**, 1–11.
- 15 V. L. Sushkevich, V. V. Ordonsky and I. I. Ivanova, *Catal. Sci. Technol.* 2016, **6**, 6354–6364.
- 16 Z. Fei, S. Ai, Z. Zhou, X. Chen, J. Tang, M. Cui and X. Qiao, *Ind. Eng. Chem.* 2014, **20 (6)**, 4146–4151.
- 17 Y. Yoshida and Y. Yamamoto, U.S. Patent 4,028,424 1977
- 18 A.M. Hawkins, U.S. Patent 4,052,478 1977
- 19 P. Li, Y. Zhang, J. Liu, L. Cui, Sh. Cao, J. Pang, L. Li and Y. Li, CN103804145B 2016
- 20 W. Hao, X. Ma, J. Qiu, J. Meng and Sh. Huang, CN104387234B 2016
- 21 E. S. Vasiliadou, N. S. Gould and R. F. Lobo, *ChemCatChem*, 2017, **9**, 4417–4425.
- 22 Ch. Baerlocher and L. B. McCusker, Database of Zeolite Structures. <http://www.iza-structure.org/databases/>.
- 23 Y. Zhao and D. G. Truhlar, *Theor. Chem. Acc.* 2008, **120 (1–3)**, 215–241.
- 24 A. K. Rappé, C. J. Casewit, K. S. Colwell, W. A. Goddard and W. M. Skiff, *J. Am. Chem. Soc.* 1992, **114 (25)**, 10024–10035.
- 25 S. Dapprich, I. Komáromi, K. S. Byun, K. Morokuma and M. J. Frisch, *J. Mol. Struct. THEOCHEM* 1999, **461–462**, 1–21.
- 26 M. J. Frisch, *J. Comput. Chem.*, 2003, **24**, 760–769.
- 27 R. E. Patet, S. Caratzoulas and D. G. Vlachos, *Phys. Chem. Chem. Phys.* 2016, **18 (37)**, 26094–26106.
- 28 R. E. Patet, W. Fan, D. G. Vlachos and S. Caratzoulas, *ChemCatChem* 2017, **9 (13)**, 2523–2535.
- 29 R. E. Patet, S. Caratzoulas and D. G. Vlachos, *J. Phys. Chem. C* 2017, **121 (40)**, 22178–22186.
- 30 R. E. Patet, M. Koehle, R. F. Lobo, S. Caratzoulas and D. G. Vlachos, *J. Phys. Chem. C* 2017, **121 (25)**, 13666–13679.
- 31 T. Salavati-Fard, S. Caratzoulas, R. F. Lobo and D. J. Doren, *ACS Catal.* 2017, **7 (3)**, 2240–2246.
- 32 D. R. Adams and S. P. Bhatnagar, *Synthesis (Stuttg)*. 1977, **10**, 661–672.
- 33 C. Angelici, B. M. Weckhuysen and P. C. A. Bruijninx, *ChemSusChem* 2013, **6**, 1595 – 1614.
- 34 P. P. Peralta-Yahya, F. Zhang, S. B. Del Cardayre and J. D. Keasling, *Nature* 2012, **488 (7411)**, 320–328.
- 35 N. Ichikawa, S. Sato, R. Takahashi and T. Sodesawa, *J. Mol. Catal. A Chem.* 2006, **256 (1–2)**, 106–112.

- 36 W. Vermeiren and F. Bouvart, US20110040133A1 2009.
- 37 Zh. Zhixin, W. Yehong, L. Jianmin, Zh. Chaofeng, W. Min, Li. Mingrun, L. Xuebin and W. Feng, *ACS Catal.* 2016, **6**, 8248–8254.
- 38 H. M. R. Hoffmann, *Angew. Chem. Int. Ed.* 1969, **8 (8)**, 556–577.
- 39 K. Fukui, *Science* 1982, **218**, 747–754.
- 40 M. Yamanaka and K. Mikami, *Helv. Chim. Acta* 2002, **85 (12)**, 4264–4271.
- 41 Q. Yang, X. Tong and W. Zhang, *J. Mol. Struct. THEOCHEM* 2010, **957 (1–3)**, 84–89.
- 42 S. Wannakao, P. Khongpracha and J. Limtrakul, *J. Phys. Chem. A*, 2011, **115 (45)**, 12486–12492.
- 43 H. Fu, S. Xie, A. Fu and T. Ye, *Comput. Theor. Chem.*, 2012, **982**, 51–57.
- 44 O. Y. Kupova, I. V. Vakulin, R. F. Talipov, N. D. Morozkin and G. R. Talipova, *React. Kinet. Mech. Catal.* 2013, **110 (1)**, 41–52.
- 45 Q. Deng, B. E. Thomas, K. N. Houk and P. Dowd, *J. Am. Chem. Soc.* 1997, **119 (29)**, 6902–6908.
- 46 A. G. Leach, K. N. Houk and C. S. Foote, *J. Org. Chem.* 2008, **73 (4)**, 8511–8519.
- 47 X. Hong, B. M. Trost and K. N. Houk, *J. Am. Chem. Soc.* 2013, **135 (17)**, 6588–6600.
- 48 S. Van de Vyver, C. Odermatt, K. Romero, T. Prasomsri and Y. Román-Leshkov, *ACS Catal.* 2015, **5**, 972–977.
- 49 J. T. Hynes, In *Hydrogen-Transfer reactions*; James T. Hynes, Judith P. Klinman, Hans-Heinrich Limbach, & R. L. S., Ed.; 2007; pp 303–349.
- 50 S. Kozuch and J. M. L. Martin, *ACS Catal.* 2012, **2 (12)**, 2787–2794.
- 51 S. Kozuch and S. A Shaik, *J. Am. Chem. Soc.* 2006, **128 (10)**, 3355–3365.
- 52 S. Kozuch and S. Shaik, *Acc. Chem. Res.* 2011, **44 (2)**, 101–110.

Graphical Abstract:

H-ZSM-5 was identified as the most efficient catalyst for the liquid phase Prins condensation of formaldehyde with isobutene to 3-methyl-3-buten-1-ol and subsequently isoprene.